Journal of Power Sources 195 (2010) 4129–4134

Contents lists available at ScienceDirect

Journal of Power Sources

journal homepage: www.elsevier.com/locate/jpowsour

Short communication

Electrocatalytic properties of carbon-supported Pt-Ru catalysts with the high alloying degree for formic acid electrooxidation

Yu Chen*, Yiming Zhou, Yawen Tang, Tianhong Lu*

College of Chemistry and Environmental Science, Nanjing Normal University, Nanjing 210097, PR China

ARTICLE INFO

Article history:
Received 26 November 2009
Received in revised form 24 January 2010
Accepted 25 January 2010
Available online 1 February 2010

Keywords:
Pt-Ru/C catalyst
Formic acid electrooxidation
Alloying degree
Bifunctional mechanism
Electronic effect

ABSTRACT

A series of carbon-supported bimetallic Pt-Ru catalysts with high alloying degree and different Pt/Ru atomic ratio have been prepared by a chemical reduction method in the H_2O/ethanol/tetrahydrofuran (THF) mixture solvent. The structural and electronic properties of catalysts are characterized using X-ray reflection (XRD), X-ray photoelectron spectroscopy (XPS), transmission electron microscopy (TEM). The electrooxidation of formic acid on these Pt-Ru nanoparticles are investigated by using cyclic voltammetry, chronoamperometry and CO-stripping measurements. The results of electrochemical measurements illustrate that the alloying degree and Pt/Ru atomic ratio of Pt-Ru catalyst play an important role in the electrocatalytic activity of the Pt-Ru/C catalyst for formic acid electrooxidation due to the bifunctional mechanism and the electronic effect. Since formic acid is an intermediate in the methanol electrooxidation on Pt electrode in acidic electrolyte, the observation provides an additional fundamental understanding of the structure–activity relationship of Pt-Ru catalyst for methanol electrooxidation.

1. Introduction

Fuel cells are electrochemical devices which convert chemical energy directly to electrical energy with high conversion efficiency and low environmental pollution [1]. Over the past few decades, the electrooxidation of methanol has received great attention owing to the potential application in direct methanol fuel cells (DMFCs), which shows great potential as high efficiency, low-emission future power source [2]. However, the low anode performance is one of the major challenges in the commercialization of DMFCs, which mainly originates from the strong adsorption of poisonous intermediates (e.g. CO) on the catalyst surface and the resulting impeded accessibility of the catalytic sites by methanol molecules [1,3]. In order to minimize the self-poisoning of catalyst, various Pt-based alloy catalysts, such as Pt-Ru, Pt-Ir, Pt-Sn, Pt-Bi, Pt-Pb, Pt-Os and Pt-Mo, have been prepared and evaluated in the electrocatalytic oxidation of methanol. Among them, the Pt-Ru binary catalyst is currently the most important anode catalyst for DMFCs because Pt-Ru alloy catalyst can show an enhanced CO electrooxidation kinetics compared to pure Pt catalyst [4,5]. The promotion effect of Ru in the Pt-Ru catalyst can be attributed to the bifunctional mechanism and the electronic effect induced by the electronic interaction between Pt and Ru, enhancing the oxidation of the adsorbed CO intermediate at the Pt surface by weakening the metal–CO bond [6,7].

Up to date, a lot of works have been devoted to study the relationship between the structure of Pt-Ru catalyst and activity of Pt-Ru catalyst. It is observed that the electrocatalytic activity of the Pt-Ru/C catalyst for methanol electrooxidation is strongly dependent on the component, particle size and morphology, and so forth [4,8,9]. However, there exists controversy regarding the effect of the alloying degree on the electrocatalytic activity of Pt-Ru catalyst [10–13]. During process of methanol electrooxidation, spectra experiments have shown that CO, formic acid, formaldehyde, etc., are intermediates in the oxidation of methanol on a Pt electrode [14]. Since formic acid is an intermediate in the methanol electrooxidation on Pt electrode in acidic electrolyte, it will be interesting to study the electrooxidation of formic acid on the Pt-Ru catalysts, which will provide an additional fundamental understanding of the structure–activity relationship of Pt-Ru catalyst for methanol electrooxidation.

Although formic acid is an intermediate in the methanol electrooxidation, the effect of structure and component of Pt-Ru catalyst on the formic acid electrooxidation seems to be ignored. The effect of these factors on formic acid electrooxidation is still not well understood. Until now, very rare investigations are known in the literature dealing with the influence of the alloying degree and Pt/Ru atomic ratio on formic acid electrooxidation [15]. In the present paper, based on our previous work [16], we synthesize a series of Pt-Ru/C catalysts with the high alloying degree and different Pt/Ru atomic ratio in the H_2O/ethanol/tetrahydrofuran (THF) mixture solution by a simple chemical reduction method. The performance of the prepared Pt-Ru/C catalysts for formic acid electrooxidation is monitored and compared with that of a commercial Pt-Ru/C cat-

* Corresponding authors. Tel.: +86 25 85891651; fax: +86 25 83243286.
E-mail addresses: ndchenyu@yahoo.cn (Y. Chen), tianhonglu@263.net (T. Lu).

0378-7753/$ – see front matter © 2010 Elsevier B.V. All rights reserved.
doi:10.1016/j.jpowsour.2010.01.054

alyst with the low alloying degree. The results of electrochemical measurements illustrate that the alloying degree and Pt/Ru atomic ratio of Pt-Ru/C catalyst can affect significantly the electrocatalytic activity of the Pt-Ru/C catalyst for formic acid electrooxidation.

2. Experimental

2.1. Preparation of carbon-supported bimetallic Pt-Ru catalysts

All chemical reagents are analytical grade. $H_2PtCl_6{\cdot}6H_2O$, $RuCl_3$, tetrahydrofuran (THF) and ethanol were obtained from Shanghai Chemical Regent Ltd. Vulcan XC-72 carbon (XC-72) was obtained from Cabot Company. In order to obtain carbon-supported bimetallic Pt-Ru catalyst (Pt-Ru/C) with 20 wt.% Pt-Ru and the different Pt/Ru atomic ratio, 60 mg Vulcan Carbon XC-72, appropriate amounts of aqueous solution of H_2PtCl_6 and $RuCl_3$, THF, CH_3CH_2OH and H_2O were mixed. To this mixture, volume ratio of $THF/H_2O/CH_3CH_2OH$ is 5:4:1 and total volume of solution is 12 mL. After the mixture solution was ultrasonicated for 1 h and mechanically stirred for 19 h, 10 mL $THF/H_2O/CH_3CH_2OH$ mixture solution (volume ratio of $THF/H_2O/CH_3CH_2OH$ is 5:4:1) containing $NaBH_4$ and Na_2CO_3 was added to the solution and stirred for 1 h at 10 °C. Then, it was filtered and washed with the triply distilled water and ethanol. Finally, it was dried in a vacuum oven at 60 °C. The homemade 20 wt.% Pt-Ru/C catalysts with the atomic ratio of Pt/Ru = 1:1, 2:1 and 3:1 were noted as the Pt_1Ru_1/C, Pt_2Ru_1/C and Pt_3Ru_1/C catalysts, respectively. For comparison, the commercial E-TEK Pt-Ru/C catalyst with 20 wt.% Pt-Ru and the atomic ratio of Pt/Ru = 1:1 was noted as the Pt_1Ru_1/C-E catalyst. EDX measurements showed the metal loadings of all catalysts in this study were about 19.8 wt.%.

2.2. Physical characterization of catalysts

The composition of the Pt-Ru/C catalyst was determined with energy-dispersive X-ray (EDX) analysis with Vantage Digital Acquisition Engine (Thermo Noran, USA), using the commercial Pt_1Ru_1/C-E catalysts as a reference on various spots of a measured sample in order to estimate average composition of the Pt_1Ru_1/C, Pt_2Ru_1/C and Pt_3Ru_1/C catalysts. The morphology and particle size of Pt-Ru/C catalysts were investigated using a JEOL JEM-2010 transmission electron microscope (TEM) operated at 200 kV accelerating potential. The X-ray diffraction (XRD) patterns for the catalysts were obtained on a Model D/max-rC X-ray diffractometer with the Cu Kα (λ = 1.5406 Å) radiation source operating at 40 kV and 100 mA. X-ray photoelectron spectroscopy (XPS) measurements were carried out on a Kratos XSAM-800 spectrometer with an Mg Kα radiator, and the vacuum in the analysis chamber was maintained at about 10^{-9} mbar or lower. Detailed Pt 4f signals were collected and analyzed. The binding energy was calibrated by means of the C 1s peak energy of 284.6 eV.

2.3. Electrochemical measurements

The electrochemical measurements were performed in a conventional three-electrode electrochemical cell by using a CHI 600 electrochemical analyzer (CH Instruments, Shanghai Chenghua Co.). A Pt plate auxiliary electrode and a saturated calomel reference electrode (SCE) were used. All potentials refer to SCE. For preparation of Pt-Ru/C working electrode, typical process follows the previous procedure reported [16]. Briefly, a glassy carbon electrode was polished with 0.3 and 0.05 μm Al_2O_3 sequentially and washed. 8 mg Pt-Ru/C catalyst and 3.25 mL mixture solution of 20% C_2H_5OH + 73.75% H_2O + 6.25% Nafion (5 wt.%) were mixed and sonicated for 30 min. 4 μL slurry obtained was placed on the surface of the glassy carbon electrode with 3 mm diameter. After drying, the working electrode was obtained. The apparent surface area of the glassy carbon electrode is 0.07 cm^2 and the specific loading of Pt-Ru on the electrode surface is about 28 μg cm^{-2}. All the electrochemical measurements were carried out at 36 ± 1 °C. The electrolyte was purged with high-purity nitrogen for at least 15 min prior to measurements to remove dissolved oxygen unless otherwise stated. For CO-stripping measurements, the catalyst surface was firstly saturated with CO by bubbling CO through 0.5 M H_2SO_4 solution while holding the working electrode at 0 V for 15 min. The remaining CO was purged by flowing N_2 for 30 min before measurements were made.

3. Results and discussion

3.1. EDX and TEM measurements

The particle size and composition of the Pt-Ru/C were analyzed by EDX and TEM measurements. The EDX analysis indicate that the atomic ratio of Pt and Ru in the Pt_1Ru_1/C, Pt_2Ru_1/C, Pt_3Ru_1/C and Pt_1Ru_1/C-E catalysts are 49:51, 64:36, 73:27 and 49:51 (data not shown), respectively, which agrees well with the starting stoichiometric ratio of the metals. Fig. 1 shows the TEM images of the homemade Pt-Ru/C catalysts and the commercial Pt_1Ru_1/C-E catalyst. It is observed that Pt-Ru particles are highly dispersed uniformly on the carbon support, and have similar morphology. The average sizes of the Pt-Ru particles, d_{TEM}, in the Pt_1Ru_1/C, Pt_2Ru_1/C, Pt_3Ru_1/C and Pt_1Ru_1/C-E catalysts are 3.0, 3.2, 3.3 and 2.8 nm, respectively, indicating that the size of the Pt-Ru particle increases slightly with the decrease of Ru content in the homemade catalysts. When PtRu/C catalyst with 20 wt.% Pt-Ru and the atomic ratio of Pt/Ru = 1:1 was synthesized by the same method in the absence of THF, the size of the Pt-Ru particle in the PtRu/C catalyst is 8.4 nm [16] (data not shown). Thus, the present results of TEM images indicate that the existence of THF can effectively prevent agglomeration of Pt-Ru particles and facilitate the dispersion of Pt-Ru particles on the carbon support. In the previous works, Prabhuram et al. found THF could acts as an excellent dispersing medium for the metal particles [17]. Recently, Shi and coworkers observed that a large numbers of neutral $(THF)_n(H_2O)_m$ (n = 2–5, m = 0–n − 1) clusters

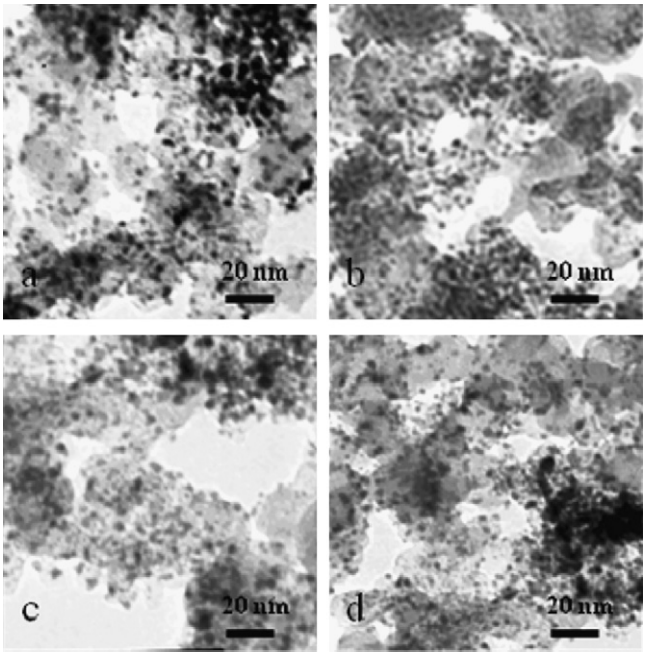

Fig. 1. TEM images of (a) Pt_1Ru_1/C, (b) Pt_2Ru_1/C, (c) Pt_3Ru_1/C and (d) Pt_1Ru_1/C-E catalysts.

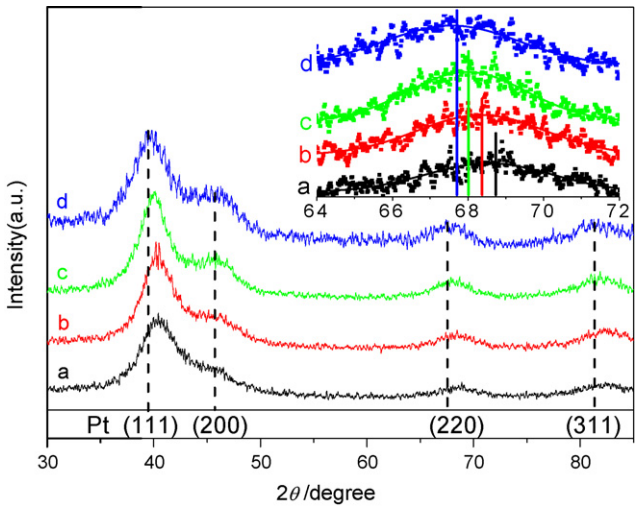

Fig. 2. XRD patterns of (a) Pt_1Ru_1/C, (b) Pt_2Ru_1/C, (c) Pt_3Ru_1/C and (d) Pt_1Ru_1/C-E catalysts. Insert: Gaussian fitting curves of Pt (2 2 0) peak of corresponding Pt-Ru/C catalysts.

molecule lay in the THF/H_2O binary system by using the molecular beam and synchrotron radiation mass spectrometry technique [18]. Probably, the tremendous neutral $(THF)_n(H_2O)_m$ clusters molecule may effectively prevent agglomeration of metal particle due to steric hindrance effect.

3.2. XRD and XPS measurements

The structures of all Pt-Ru/C catalysts were investigated by XRD. Fig. 2 shows the XRD patterns of homemade Pt_1Ru_1/C, Pt_2Ru_1/C, Pt_3Ru_1/C and commercial Pt_1Ru_1/C-E catalysts. Four characteristic peaks corresponding to (1 1 1), (2 0 0), (2 2 0) and (3 1 1) planes of the face centered cubic (*fcc*) structure of pure Pt are observed in each XRD patterns. The diffraction peaks of all Pt-Ru/C catalysts are shifted to higher 2θ value comparing with the peak position of the pure Pt (JCPDS card 04-0802), indicating that Ru has entered into Pt lattice and the alloy of Pt and Ru is formed. No visible peaks related to tetragonal RuO_2 or hexagonal close-packed (*hcp*) Ru phases were found in Fig. 2, but their presence cannot be discarded because they may be present in a small amount or even in an amorphous form [19].

In order to avoid disturbance of the diffraction peak of the carbon support, Pt (2 2 0) diffraction peak was fitted using the Gaussian function to obtain precisely the position of the peak maximum ($2\theta_{max}$) (insert in Fig. 2). The particle size (d_{XRD}), the lattice parameters (a) and the atomic fraction of Ru in the alloy (χ_{Ru}) of Pt-Ru/C catalysts were calculated using Pt (2 2 0) diffraction peak with Scherrer's formula [20], Vegard's law [21] and Antolini's equation [22], respectively, and the results are listed in Table 1. As shown in Table 1, the atomic fraction of Ru in the alloy of Pt_1Ru_1/C catalyst (χ_{Ru} = 44.2 at.%) is very close to the EDX compositions of Pt_1Ru_1/C catalyst (atomic ratio of Pt and Ru is 49:51), indicating almost all Ru atom entered into Pt lattice to form Pt-Ru alloy, and the alloying degree of homemade Pt_1Ru_1/C catalyst is much higher than that of commercial Pt_1Ru_1/C-E catalyst (χ_{Ru} = 4.4 at.%). In our previous work [16], we have found that the reduction potentials of H_2PtCl_6 and $RuCl_3$ in the solution containing THF are similar due to the formation of H_2PtCl_6-THF complex, which can results in simultaneous reduction of H_2PtCl_6 and $RuCl_3$, and subsequent formation of Pt-Ru/C catalyst with high alloying degree. The versatility of preparation method is further confirmed by XRD measurements of other homemade Pt-Ru/C samples. As shown in Fig. 2, the Pt (2 2 0) reflection in homemade Pt-Ru/C catalyst orderly shifts to lower 2θ values with decrease of the Ru content. The results in Table 1 confirm that χ_{Ru} in each homemade Pt-Ru/C catalyst is very close to their EDX compositions, indicating almost all Ru atom entered into Pt lattice to form Pt-Ru alloy in each homemade Pt-Ru/C catalyst. This further demonstrates that the atomic ratio of Pt to Ru in the synthesized catalysts can be adjusted with the present method.

Generally, the addition of Ru to Pt can lead to a change of the electronic structure of Pt atom due to lattice strain and charge transfer [23–25]. Since the average size of Pt-Ru particles in Pt_1Ru_1/C and Pt_1Ru_1/C-E catalysts are similar (Table 1), the effect of particle size on binding energy (BE) of Pt can be ruled out [26,27]. Compared with the commercial Pt_1Ru_1/C-E catalyst, the homemade Pt_1Ru_1/C catalyst have a +0.5 eV increase in binding energy of Pt^0 $4f_{7/2}$ (Table 1), which should be mainly caused by a stronger electronic interaction between Pt and Ru atoms in Pt_1Ru_1/C catalyst due to a higher alloying degree, leading to a obvious decrease of the electron density of Pt atom in Pt_1Ru_1/C catalyst. Except that the alloying degree of Pt-Ru particle affects the binding energy of Pt^0 $4f_{7/2}$, the atomic composition of Pt-Ru/C catalyst makes an effect on the binding energy of Pt^0 $4f_{7/2}$. As shown in Table 1, the Pt^0 $4f_{7/2}$ binding energy in homemade Pt-Ru/C catalysts orderly increases with increasing Ru content. Although the Ru content of Pt_3Ru_1/C catalyst is much lower than that of commercial Pt_1Ru_1/C-E catalyst, the binding energy of Pt^0 $4f_{7/2}$ in the Pt_3Ru_1/C catalyst is higher than that of Pt_1Ru_1/C-E catalyst (Table 1), which in turn confirms again that the alloying degree of Pt-Ru particle makes a significant effect on the binding energy of Pt^0 $4f_{7/2}$.

3.3. Hydrogen adsorption/desorption measurements

Fig. 3 shows the cyclic voltammograms (CVs) of Pt_1Ru_1/C, Pt_2Ru_1/C, Pt_3Ru_1/C and Pt_1Ru_1/C-E catalysts in a 0.5 M H_2SO_4 solution. The upper limit of the CVs is 0.5 V to prevent any Ru dissolution [28]. Obviously, the electrochemical characteristic curves of the homemade Pt-Ru/C catalysts in 0.5 M H_2SO_4 depend on the composition of Pt and Ru. With increasing Ru component in the homemade Pt-Ru/C catalysts, the thickness of the double layer region, at the potential range of 0.1–0.5 V, is increased due to the hydrophilic properties of Ru [29–31]. Meanwhile, the features in the "hydrogen region", at the potential range of −0.2 to 0.1 V, gradually begins to resemble the features of pure Pt with decreasing Ru component in the homemade Pt-Ru/C catalysts. This further demonstrates that the atomic ratio of Pt to Ru in the synthesized catalysts can be adjusted with the present method. Although the electrochemically active surface of Pt-Ru/C catalyst cannot be precisely assessed by coulometry in the "hydrogen region" due to the overlap of hydrogen desorption on Pt surface and the formation of Ru oxide, it can be concluded from Fig. 3 that the order of the amount of Pt site in three homemade Pt-Ru/C

Table 1
The structural parameters of the different Pt-Ru/C catalysts.

Catalyst	d_{XRD} (nm)	d_{TEM} (nm)	$2\theta_{max}$ (°)	a (nm)	Pt/Ru atomic ratio from EDX (%)	x_{Ru} (%)	Pt^0 $4f_{7/2}$ BE (eV)
Pt_1Ru_1/C	2.7	3.0	68.70	0.38606	49:51	44.2	71.3
Pt_2Ru_1/C	3.0	3.2	68.40	0.38755	64:36	32.3	71.2
Pt_3Ru_1/C	3.2	3.3	68.12	0.38894	73:27	21.0	71.0
Pt_1Ru_1/C-E	2.6	2.8	67.72	0.39097	49:51	4.4	70.8

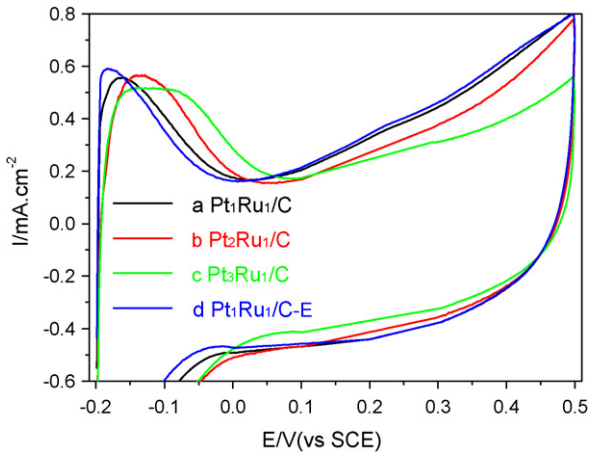

Fig. 3. The cyclic voltammograms of (a) Pt_1Ru_1/C, (b) Pt_2Ru_1/C, (c) Pt_3Ru_1/C and (d) Pt_1Ru_1/C-E catalysts in the 0.5 M H_2SO_4 solution at the rate of 50 mV s^{-1} after 1 potential cycles.

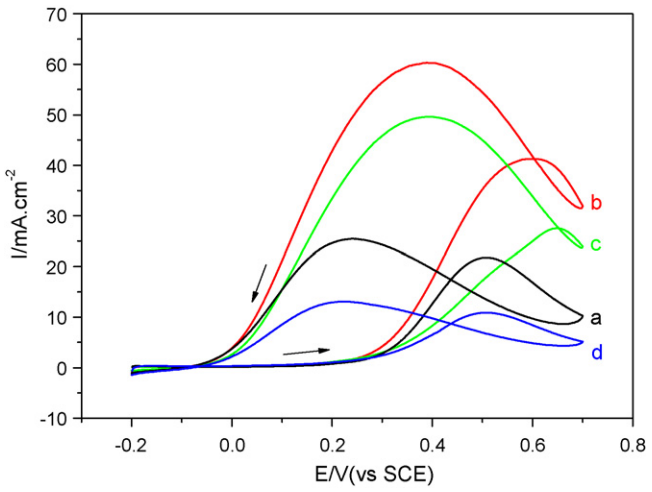

Fig. 4. Cyclic voltammograms of the 0.5 M H_2SO_4 + 0.5 M HCOOH solution at (a) Pt_1Ru_1/C, (b) Pt_2Ru_1/C, (c) Pt_3Ru_1/C and (d) Pt_1Ru_1/C-E catalysts at the rate of 50 mV s^{-1} after 1 potential cycles.

catalysts is $Pt_3Ru_1/C > Pt_2Ru_1/C > Pt_1Ru_1/C$ because the hydrogen region features of Pt gradually enhance with decreasing Ru component. Another significant observation is that the electrochemical characteristic curve of Pt_1Ru_1/C catalyst is similar to that of the commercial Pt_1Ru_1/C-E catalyst, indicating that the amount of Pt site in Pt_1Ru_1/C catalyst is similar to that of the commercial Pt_1Ru_1/C-E catalyst.

3.4. Electrooxidation of formic acid

Formic acid electrooxidation obeys a triple-path mechanism in acidic electrolyte [32,33] (Scheme 1), namely: (i) a direct pathway (dehydrogenation), in which formic acid is oxidized directly into CO_2; (ii) an indirect pathway (dehydration), via CO_{ads} formation and oxidation; (iii) a formate pathway, involving the formation and subsequent oxidation of formate to CO_2. Fig. 4 shows the cyclic voltammograms of 0.5 M HCOOH + 0.5 M H_2SO_4 solution at four different Pt-Ru/C catalysts. In the positive scan direction, a broad oxidation current peak is observed in each of the cyclic voltammograms, which should be overlap of the formic acid oxidation peak via different reaction path. During the positive potential scan, some products of HCOOH adsorption decomposition may lead to a Pt-site blocking effect, which inhibits access of HCOOH molecules to the Pt active sites [14,34,35]. In the reverse scan direction, an oxidation peak is also observed in each of the cyclic voltammograms, which is assigned to the direct oxidation of formic acid. This oxidation peak can present the real catalytic activity of the Pt surface, since neither CO nor Pt oxides are present in the catalyst surface [14,34,35]. As a result, in each of the cyclic voltammograms, it is observed that the oxidation peak current of formic acid in the reverse scan direction is bigger than that in the positive scan direction. Because the thickness of a diffusion layer decreases with the increase of the stirring rate, the rate of a diffusion-controlled reaction depends on the

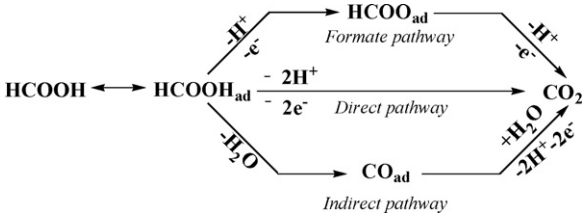

Scheme 1. Schematic description of the "triple-path way" reaction mechanism for formic acid oxidation as proposed in refs. [32] and [33].

stirring rate of a solution. Under continuous stirring condition, the cyclic voltammograms of formic acid at Pt-Ru/C catalysts give the same curve as the one in the static solution in Fig. 4. The fact indicates that the oxidation of formic acid at the Pt-Ru/C catalysts is not a diffusion-controlled reaction rather than a kinetic-controlled reaction.

To evaluate the electrocatalytic activity of Pt-Ru/C catalysts for formic acid electrooxidation, two electrochemical parameters must be taken into consideration: the onset oxidation potential of fuel molecules and the magnitude of the oxidation current density at a given potential in the positive scan direction [36]. For the electrooxidation of formic acid, all Pt-Ru/C catalysts exhibit onset potentials of ca. 0.25 V (Table 2), indicating the onset oxidation potential of formic acid on Pt-Ru/C catalyst is not related to the degree of alloying and Pt/Ru atomic ratio of Pt-Ru/C catalyst under the present experimental conditions (i.e. the Pt/Ru atomic ratio $\leq$ 3:1). In order to investigate the effect of alloying degree on formic acid electrooxidation, we firstly compare the electrocatalytic activity of Pt_1Ru_1/C and Pt_1Ru_1/C-E catalyst for formic acid electrooxidation. As shown in Fig. 4, the oxidation peak potentials of formic acid at the Pt_1Ru_1/C and Pt_1Ru_1/C-E catalysts are almost the same in the positive scan direction, at about 0.51 V. However, the anodic peak current density of formic acid at the Pt_1Ru_1/C catalyst (21.8 mA cm^{-2}) is much bigger than that of Pt_1Ru_1/C-E catalyst (10.9 mA cm^{-2}). Considering that the component and the average size of Pt-Ru particle in the Pt_1Ru_1/C and Pt_1Ru_1/C-E catalysts are similar, but x_{Ru} of the Pt_1Ru_1/C catalyst is much higher than that of the Pt_1Ru_1/C-E catalyst, it can be concluded that the alloying degree of Pt-Ru particles is an important factor to affect the electrocatalytic activity of the Pt-Ru/C catalyst for the formic acid electrooxidation.

The positive shift in the Pt 4f binding energy corresponds to a shift of the center of the d-band toward higher binding energy, leading to a downshift in the center of gravity of the d-band of Pt with respect to the Fermi level [15]. The previous the d-band center theory has indicated that a change in the adsorbate chemisorption energy scales directly with the change in the metal center of the d-band: lowering of the d-band center results in the decrease in interaction strength of the various adsorbates to the substrate [37,38]. Consequently, the activity of a catalyst can be tuned by changing the electronic structure of metal center. As mentioned, formic acid electrooxidation obeys a triple-path mechanism. During the electrooxidation of formic acid, at low potentials, adsorbed CO produced from formic acid decomposition is the inhibiting intermediate [1,3]. At higher potentials, formate inter-

Table 2
Onset potentials, peak potential and current densities of formic acid oxidation at Pt_1Ru_1/C, Pt_2Ru_1/C, Pt_3Ru_1/C and Pt_1Ru_1/C-E catalysts at different voltages.

Catalyst	Onset potential (V)	Peak potential (V)	Current density ($mA\,cm^{-2}$)				
			0.3 V	0.35 V	0.4 V	0.45 V	0.5 V
Pt_1Ru_1/C	0.25	0.51	2.8	6.5	12.6	18.8	21.7
Pt_2Ru_1/C	0.25	0.59	4.2	9.4	17.5	27.1	35.2
Pt_3Ru_1/C	0.25	0.65	3.0	5.1	8.3	12.5	18.1
Pt_1Ru_1/C-E	0.25	0.51	2.4	4.1	6.5	9.4	10.8

mediate is the poisoning species [39,40]. Thus, the suppression of dehydration pathway and formate pathway can enhance the rate of formic acid electrooxidation. Since the binding energy of Pt_{4f} in the Pt_1Ru_1/C catalyst is much higher than that in the Pt_1Ru_1/C-E catalyst (Table 1), this corresponding downshift in the d-band center of Pt can result in weaker bonds between the Pt surface and the adsorbate (i.e. the formate and CO_{ads} intermediates in Scheme 1). In turn, this indicates that the activation barrier energy of the various adsorbates to the substrate increases (surface activation of various adsorbates becomes more difficult), which will decrease the formation of the formate and CO_{ads} intermediates. In the case of Pd catalyst, Wieckowsk and co-workers have confirmed that the lower d-band center of Pd results in an increase in activation barrier energy of the formate and CO_{ads} intermediates, which enhances the rate of the formic acid oxidation via the direct path [23]. Similarly, Pt_1Ru_1/C catalyst with high alloying degree may enhance the rate of the formic acid oxidation by suppressing indirect pathway and formate pathway of formic acid oxidation due to an increase in activation barrier energy of the formate and CO_{ads} intermediates, which result in a better electrocatalytic activity of the Pt_1Ru_1/C catalyst for the formic acid electrooxidation compared to Pt_1Ru_1/C-E catalyst.

Similar to the case of methanol electrooxidation [15], it is observed that the atomic compositions of Pt-Ru/C catalyst affect also the electrocatalytic activity of the Pt-Ru/C catalyst for formic acid electrooxidation. As shown in Fig. 4, the forward peak potentials of formic acid oxidation at homemade Pt-Ru/C catalysts orderly increases with decreasing Ru content, while the peak currents of formic acid oxidation at homemade Pt-Ru/C catalysts display a volcano change with decreasing Ru content. Table 2 lists also the anodic current densities of formic acid at several potentials for the four Pt-Ru/C catalysts. These values can reflect effectively the electrocatalytic activity of catalyst [36]. Analysis of Table 2 reveals that Pt_2Ru_1/C catalyst has highest electrocatalytic activity for formic acid oxidation among the four samples. For example, at 0.3 and 0.5 V, Pt_2Ru_1/C catalyst exhibit current densities that are about 1.8 and 3.5 times higher compared to commercial Pt_1Ru_1/C-E catalyst, respectively. In comparison with the result of the hydrogen adsorption/desorption measurements (i.e. the amount of Pt site in three homemade Pt-Ru/C catalysts is Pt_3Ru_1/C > Pt_2Ru_1/C > Pt_1Ru_1/C), the present result indicates that the appropriate Pt/Ru atomic ratio plays an important role in the electrocatalytic activity of the Pt-Ru/C catalyst for the formic acid electrooxidation.

The electrocatalytic activity and stability of the different Pt-Ru/C catalysts were further tested by chronoamperometry (Fig. 5). It is observed that the oxidation current densities of formic acid at Pt_1Ru_1/C, Pt_2Ru_1/C, Pt_3Ru_1/C and Pt_1Ru_1/C-E catalyst electrodes at 3000 s are 4.4, 6.7, 2.8 and 2.2 $mA\,cm^{-2}$, corresponding to 45%, 47%, 28% and 30% of their initial maximum values, respectively. The results show that the order of the electrocatalytic activity of the Pt-Ru/C catalysts for the formic acid electrooxidation is the Pt_2Ru_1/C > Pt_1Ru_1/C > Pt_3Ru_1/C > Pt_1Ru_1/C-E catalyst, whereas the order of the electrocatalytic stability is the Pt_2Ru_1/C ≈ Pt_1Ru_1/C > Pt_3Ru_1/C ≈ Pt_1Ru_1/C-E catalyst. When we normalized the oxidation current of formic acid by using the Pt electrochemically active surface area of catalysts, a same change tendency is also observed (insert in Fig. 5). The excellent electrocatalytic activity of the Pt_2Ru_1/C catalyst for the formic acid oxidation may be attributed to the appropriate Pt/Ru atomic ratio and high alloying degree of the Pt-Ru particles.

3.5. Electrochemical oxidation of surface adsorbed CO

During process of formic acid electrooxidation on Pt surface, CO_{ads}, an intermediate product of formic acid oxidation will inhibit the forthcoming formic acid electrooxidation by preventing their adsorption at the electrode surface, which will inevitably decrease the fuel efficiency. The alloying of Pt with other metals like Ru has been tested as a way of minimizing the effect of poisonous intermediates, in which Ru can promote the oxidation of the strongly bound CO_{ads} on Pt by supplying an oxygen source (Ru-OH_{ad}) at lower potentials than Pt [8,9,41]. Moreover, the Pt-Ru alloy is emphasized because the possible electronic effect between Pt and Ru atoms is also thought to be important, which can reduce the bonding strength between Pt and CO_{ads}, and thus benefit the catalysis [8,9,41]. As shown in Fig. 6, the oxidation peak potentials of adsorbed CO at Pt_1Ru_1/C and Pt_1Ru_1/C-E samples are 0.306 and 0.388 V, respectively, illustrating the adsorption strength of the adsorbed CO on the Pt-Ru/C catalysts is related to the alloying degree of Pt-Ru. Obviously, the Pt-Ru/C catalyst with the high alloying degree is favor of oxidation of CO_{ads}. Consequently, the electrocatalytic stability of the Pt_1Ru_1/C catalyst for the formic acid oxidation is much better than that of the Pt_1Ru_1/C-E catalyst (Figs. 4 and 5). Since the particles size and composition of the Pt_1Ru_1/C catalyst is similar to that of the commercial Pt_1Ru_1/C-E catalyst, the effect of Ru content and particles size on CO_{ads} oxi-

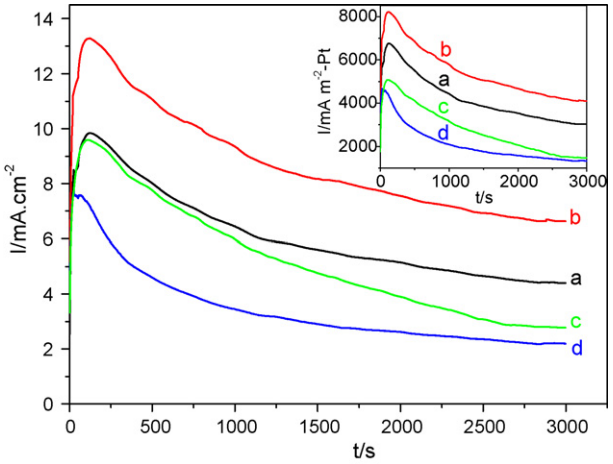

Fig. 5. Chronoamperometric curves of the 0.5 M H_2SO_4 + 0.5 M HCOOH solution at (a) Pt_1Ru_1/C, (b) Pt_2Ru_1/C, (c) Pt_3Ru_1/C and (d) Pt_1Ru_1/C-E catalysts. Fixed potential: 0.35 V. The insert shows the chronoamperometric curves normalized using the Pt electrochemically active surface area ($mA\,m^{-2}$ Pt). The electrochemically active surface areas of the Pt in catalysts are estimated from the integrated CO_{ad} oxidation charge in Fig. 6.

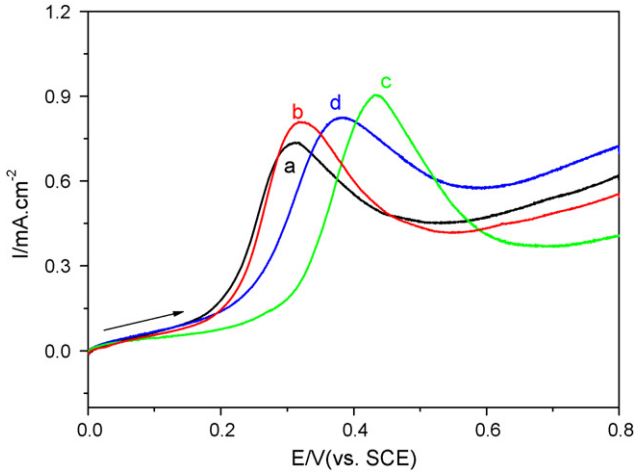

Fig. 6. The first anode scan in cyclic voltammograms for CO oxidation at (a) Pt_1Ru_1/C, (b) Pt_2Ru_1/C, (c) Pt_3Ru_1/C and (d) Pt_1Ru_1/C-E catalysts in the 0.5 M H_2SO_4 solution at the rate of 50 mV s^{-1}.

dation can be ruled out. Thus, the obvious enhancement of the CO tolerance can be ascribed to above-mentioned electronic effect.

For the homemade Pt-Ru/C catalysts with the high alloying degree, the CO_{ads}-stripping analysis (Fig. 6) demonstrate that the oxidation peak potentials of the adsorbed CO at Pt_1Ru_1/C catalyst electrode (0.306 V) is close to that of Pt_2Ru_1/C catalyst electrode (0.316 V), but much lower than that of Pt_3Ru_1/C catalyst electrode (0.431 V). According to bifunctional mechanism, adequate amount of Ru sites are required to locate close to the Pt sites to promote the conversion of CO to CO_2 on Pt surface. Thus, a significantly positive shift of the oxidation peak potentials of the adsorbed CO at Pt_3Ru_1/C catalyst is likely due to the fact that the amount of Ru in Pt_3Ru_1/C catalyst cannot afford enough oxygenated species to guarantee oxidation of CO. In addition, XPS measurements show the binding energy values of Pt_{4f} in homemade Pt-Ru/C catalysts decrease with decreasing Ru content (Table 1), which is an indication of weakening of interaction between Pt and Ru atom. Consequently, the weakening of electronic effect originated from the decrease of amount of Ru in Pt_3Ru_1/C catalyst is also likely responsible for the positive shift of the oxidation peak potentials of the adsorbed CO. In summary, the decrease of CO tolerance is main reason for the weak electrocatalytic stability of the Pt_3Ru_1/C catalyst.

4. Conclusion

The electrocatalytic activity of Pt-Ru/C catalyst for the formic acid electrooxidation reaction is strongly dependent on alloying degree and the Ru content of Pt-Ru/C catalyst. Although composition and particle size of homemade Pt_1Ru_1/C catalyst are similar to that of commercial Pt_1Ru_1/C-E catalyst, the Pt_1Ru_1/C catalyst with high alloying degree shows much higher electrocatalytic activity and stability for the formic acid electrooxidation as compared to the commercial Pt_1Ru_1/C-E catalyst with low alloying degree. This indicates that the increase of alloying degree of Pt-Ru/C catalyst is favor of formic acid electrooxidation, which can be ascribed to enhancement of CO tolerance and possible suppression of dehydration pathway and formate pathway in the course of formic acid electrooxidation due to the change of electronic structure of Pt surface. Under high alloying degree condition, it is observed that the electrocatalytic activity of Pt-Ru/C catalyst for formic acid oxidation is a volcano behavior with decreasing Ru content, where Pt_2Ru_1/C catalyst has highest electrocatalytic activity for formic acid oxidation among the three homemade Pt-Ru/C samples. Since the Pt $4f_{7/2}$ binding energy of homemade Pt-Ru/C catalyst increases with increasing Ru content, this volcano behavior cannot be explained by the electronic effect alone. Thus, it proves that the bifunctional mechanism also plays an important role in the electrocatalytic activity of the Pt-Ru/C catalyst for formic acid electrooxidation.

Acknowledgments

The authors are grateful for State Key High Technology Research Program of China (863 Program, 2007AA05Z143, 2007AA05Z159), the National Natural Science Foundation of China (20573057, 20871070), and the Priming Scientific Research Foundation for Advanced Talents in Nanjing Normal University.

References

[1] W. Chen, L.P. Xu, S.W. Chen, J. Electroanal. Chem. 631 (2009) 36.
[2] R. Chetty, W. Xia, S. Kundu, M. Bron, T. Reinecke, W. Schuhmann, M. Muhler, Langmuir 25 (2009) 3853.
[3] C.G. Lee, H. Ojima, M. Umeda, Electrochim. Acta 53 (2008) 3029.
[4] Q. Lu, B. Yang, L. Zhuang, J.T. Lu, J. Phys. Chem. B 109 (2005) 8873.
[5] E. Antolini, J. Power Sources 170 (2007) 1.
[6] F.H.B. Lima, E.R. Gonzalez, Appl. Catal. B 79 (2008) 341.
[7] Y.Y. Tong, H.S. Kim, P.K. Babu, P. Waszczuk, A. Wieckowski, E. Oldfield, J. Am. Chem. Soc. 124 (2002) 468.
[8] L. Liu, C. Pu, R. Viswanathan, Q. Fan, R. Liu, E.S. Smotkin, Electrochim. Acta 43 (1998) 3657.
[9] C. Pan, F. Dassenoy, M.J. Casanove, K. Philippot, C. Amiens, P. Lecante, A. Mosset, B. Chaudret, J. Phys. Chem. B 103 (1999) 10098.
[10] J.W. Long, R.M. Stroud, K.E. Swider-Lyons, D.R. Rolison, J. Phys. Chem. B 104 (2000) 9772.
[11] M. Koper, T. Shubina, R. Santen, J. Phys. Chem. B 106 (2002) 686.
[12] C. Roth, N. Martz, A. Morlang, R. Theissmann, H. Fuess, Phys. Chem. Chem. Phys. 6 (2004) 3557.
[13] H.A. Gasteiger, N. Markovic, P.N. Ross, E.J. Cairns, J. Electrochem. Soc. 141 (1994) 1795.
[14] J.H. Jiang, A. Kucernak, J. Electroanal. Chem. 630 (2009) 10.
[15] M.A. Rigsby, W.P. Zhou, A. Lewera, H.T. Duong, P.S. Bagus, W. Jaegermann, R. Hunger, A. Wieckowski, J. Phys. Chem. C 112 (2008) 15595.
[16] Y. Chen, Y.W. Tang, C.P. Liu, W. Xing, T.H. Lu, J. Power Sources 161 (2006) 470.
[17] J. Prabhuram, T.S. Zhao, C.W. Wong, J.W. Guo, J. Power Sources 134 (2004) 1.
[18] T.J. Shi, X. Wang, D.L. Yang, Q.H. Zhu, L.S. Sheng, G.H. Wu, Y.W. Zhang, Acta Chem. Sin. 58 (2000) 1107.
[19] F. Colmati, E. Antolini, E.R. Gonzalez, J. Power Sources 157 (2006) 98.
[20] J.B. Xu, T.S. Zhao, Z.X. Liang, J. Power Sources 185 (2008) 857.
[21] V. Radmilovic, H.A. Gasteiger, P.N. Ross, J. Catal. 154 (1995) 98.
[22] E. Antolini, F. Cardellini, J. Alloy Compd. 315 (2001) 118.
[23] W.P. Zhou, A. Lewera, R. Larsen, R.I. Masel, P.S. Bagus, A. Wieckowski, J. Phys. Chem. B 110 (2006) 13393.
[24] B. Hammer, Y. Morikawa, J.K. Nørskov, Phys. Rev. Lett. 76 (1996) 2141.
[25] P.S. Bagus, A. Wieckowski, H. Freund, Chem. Phys. Lett. 420 (2006) 42.
[26] C. Roth, M. Goetz, H. Fuess, J. Appl. Electrochem. 31 (2001) 793.
[27] D.R.M. Godoi, J. Perez, H.M. Villullas, J. Phys. Chem. C 113 (2009) 8518.
[28] L.D. Santos, F. Colmati, E.R. Gonzalez, J. Power Sources 159 (2006) 869.
[29] H.A. Gasteiger, E.J. Cairns, J. Phys. Chem. 97 (1993) 12020.
[30] K.W. Park, J.H. Choi, K.S. Ahn, Y.E. Sung, J. Phys. Chem. B 108 (2004) 5989.
[31] Y.L. Yao, Y. Ding, L.S. Ye, X.H. Xia, Carbon 44 (2006) 61.
[32] Y.X. Chen, M. Heinen, Z. Jusys, R.J. Behm, Angew. Chem. Int. Ed. 45 (2006) 981.
[33] Y.X. Chen, M. Heinen, Z. Jusys, R.J. Behm, Langmuir 22 (2006) 10399.
[34] S.G. Lemos, R.T.S. Oliveira, M.C. Santos, P.A.P. Nascente, L.O.S. Bulhoes, E.C. Pereira, J. Power Sources 163 (2007) 695.
[35] W. Chen, J.M. Kim, S.H. Sun, S.W. Chen, Langmuir 23 (2007) 11303.
[36] L.R. Alden, C. Roychowdhury, F. Matsumoto, D.K. Han, V.B. Zeldovich, H.D. Abruna, F.J. DiSalvo, Langmuir 22 (2006) 10465.
[37] B. Hammer, J.K. Norskov, Surf. Sci. 343 (1995) 211.
[38] M. Mavrikakis, B. Hammer, J.K. Norskov, Phys. Rev. Lett. 81 (1998) 2819.
[39] G.Q. Lu, A. Crown, A. Wieckowski, J. Phys. Chem. B 103 (1999) 9700.
[40] G. Samjeske, M. Osawa, Angew. Chem. Int. Ed. 44 (2005) 5694.
[41] J.M. Leger, Electrochim. Acta 50 (2005) 3123.